Calmodulin activation of Aurora-A kinase (AURKA) is required during ciliary disassembly and in mitosis

Olga V. Plotnikova[a], Anna S. Nikonova[a], Yuri V. Loskutov[b], Polina Y. Kozyulina[b], Elena N. Pugacheva[b], and Erica A. Golemis[a]

[a]Developmental Therapeutics Program, Fox Chase Cancer Center, Philadelphia, PA 19111; [b]Biochemistry Department, Mary Babb Randolph Cancer Center, West Virginia University, Morgantown, WV 26506

ABSTRACT **The centrosomal Aurora-A kinase (AURKA) regulates mitotic progression, and overexpression and hyperactivation of AURKA commonly promotes genomic instability in many tumors. Although most studies of AURKA focus on its role in mitosis, some recent work identified unexpected nonmitotic activities of AURKA. Among these, a role for basal body–localized AURKA in regulating ciliary disassembly in interphase cells has highlighted a role in regulating cellular responsiveness to growth factors and mechanical cues. The mechanism of AURKA activation involves interactions with multiple partner proteins and is not well understood, particularly in interphase cells. We show here that AURKA activation at the basal body in ciliary disassembly requires interactions with Ca^{2+} and calmodulin (CaM) and that Ca^{2+}/CaM are important mediators of the ciliary disassembly process. We also show that Ca^{2+}/CaM binding is required for AURKA activation in mitosis and that inhibition of CaM activity reduces interaction between AURKA and its activator, NEDD9. Finally, mutated derivatives of AURKA impaired for CaM binding and/or CaM-dependent activation cause defects in mitotic progression, cytokinesis, and ciliary resorption. These results define Ca^{2+}/CaM as important regulators of AURKA activation in mitotic and nonmitotic signaling.**

Monitoring Editor
Stephen Doxsey
University of Massachusetts

Received: Dec 30, 2011
Revised: Apr 19, 2012
Accepted: May 18, 2012

INTRODUCTION

The Aurora-A kinase (AURKA) is best known for roles in promoting M-phase entry and progression, where AURKA activation regulates centrosomal separation, assembly of a bipolar spindle assembly, chromosomal alignment at the metaphase plate, and cytokinesis (Marumoto *et al.*, 2005; Gautschi *et al.*, 2008). AURKA protein overexpression is observed in many cancers, where it is associated with supernumerary centrosomes, multipolar spindles, and aneuploidy, as well as a poor prognosis. Because of its oncogenic activity in tumors, AURKA has been a target of drug development, with a number of agents progressing through clinical trials and showing promising activity (Carol *et al.*, 2011; Manfredi *et al.*, 2011). However, beyond these well-established roles in mitosis and cancers, several recent studies have indicated that AURKA has additional functions in interphase cells, where it supports centrosome maturation (Hannak *et al.*, 2001; Berdnik and Knoblich, 2002), influences microtubule dynamics (Lorenzo *et al.*, 2009; Mori *et al.*, 2009; Toya *et al.*, 2011), promotes cell migration and polarity control (Wu *et al.*, 2005; Yamada *et al.*, 2010), activates the signaling proteins AKT and RALA (Yang *et al.*, 2006; Lim *et al.*, 2010; Kashatus *et al.*, 2011), induces disassembly of cilia (Pugacheva *et al.*, 2007), and regulates intracellular calcium through phosphorylation of PKD2 (Plotnikova *et al.*, 2011). Recognition of these additional functions suggests that clinical inhibitors of AURKA may have unexpected side effects. To better apply AURKA inhibitors therapeutically and better understand the biological function of AURKA, we have been studying the regulation of AURKA activity.

Most studies of AURKA activation have focused on its interaction with an activating panel of partner proteins that includes TPX2, NEDD9, AJUBA, BORA, PAK1, and others at the centrosome

This article was published online ahead of print in MBoC in Press (http://www.molbiolcell.org/cgi/doi/10.1091/mbc.E11-12-1056) on May 23, 2012.

Address correspondence to: Erica A. Golemis (EA_Golemis@fccc.edu).

Abbreviations used: AURKA, Aurora-A kinase; CaM, calmodulin; CB, Coomassie blue; CMZ, calmidazolium; Ion, ionomycin; PHA, PHA-680632.

immediately before mitosis (Bayliss *et al.*, 2003; Eyers *et al.*, 2003; Pugacheva and Golemis, 2005, 2006; Pugacheva *et al.*, 2007; Zhao *et al.*, 2005; Hutterer *et al.*, 2006). In early G1 or quiescent cells, the centrosome migrates to the cell surface and differentiates into the basal body of the cilia, an organelle that is essential for receipt of multiple classes of extracellular signals, including mechanical cues and soluble growth factors such as Hedgehog and platelet-derived growth factor α. Transient activation of AURKA at the basal body causes the cilia to resorb as cells progress through G1 to S phase (Plotnikova *et al.*, 2008). At least one of the AURKA mitotic partner proteins, NEDD9, has also been found to be important for AURKA activation at the ciliary basal body in quiescent interphase cells immediately before AURKA-dependent resorption of cilia (Pugacheva *et al.*, 2007). A second factor, PIFO, has also been suggested to support resorption-associated activation (Kinzel *et al.*, 2010), but in general, cofactors supporting activation of AURKA in interphase cells are not well understood.

AURKA contains an N-terminal, structurally disordered regulatory domain adjacent to the C-terminal kinase domain. Many of its activating partners are noncatalytic and bind to both N- and C-terminal sites on AURKA. A number of these proteins associate with AURKA in G2 phase before AURKA activation. The "switch" event permitting and timing AURKA activation by these proteins at mitotic entry is not well understood. In addition, before activation in mitosis, AURKA must escape from a series of inhibitory interactions involving proteins such as PPI, PP2A, PPTG, GADD45a, and others (reviewed in Carmena *et al.*, 2009). Although much work remains to be done, it appears that the activation process is multistep (e.g., Dodson and Bayliss, 2012) and is likely to involve allosteric reorganization of AURKA based on timed, ordered changes in interaction profile.

In this context, we recently established that interactions with calcium (Ca^{2+}) and calmodulin (CaM) in the N-terminal, structurally disordered region of AURKA provided an unexpected means of activating AURKA (Plotnikova *et al.*, 2010). However, this activation mode was observed in response to highly transient calcium stimuli, with AURKA activation and deactivation occurring within 3 min (Plotnikova *et al.*, 2010), in contrast to the much longer duration of AURKA activation observed in mitosis or ciliary resorption, which is typically 1–2 h. It was nevertheless intriguing that previous studies identified transient puffs of Ca^{2+} at the centrosome during cell cycle transitions associated with AURKA activation (reviewed in Roderick and Cook, 2008). In this study, we investigated the relationship of Ca^{2+} and CaM binding to AURKA activation in ciliary disassembly and mitosis. We find that Ca^{2+}/CaM activation of AURKA is essential for both AURKA-dependent ciliary disassembly and AURKA function in mitosis. We also find that Ca^{2+}/CaM support AURKA interactions with its activator, NEDD9, and show that targeted mutations that disrupt AURKA interactions with CaM lead to defects in mitosis and ciliary disassembly. Taken together, these findings offer new insights into control of AURKA activation.

RESULTS

Calcium influx and calmodulin activity are required for ciliary disassembly

We assessed the role of calcium in ciliary disassembly. Treatment of ciliated, quiescent hTERT-RPE1 cells with ionomycin to induce calcium influx induced robust ciliary disassembly even without the addition of serum (50% ciliated vs. 90% for dimethyl sulfoxide [DMSO]-treated cells, after 2 h). Additional disassembly was observed when serum was added (to 20% ciliated vs. 37% for serum only; Figure 1, a and b). Reciprocally, pretreatment of cells with the CaM inhibitors calmidazolium (CMZ) or W7 or the calcium chelator ethylene glycol tetraacetic acid (EGTA) completely inhibited serum-induced resorption of cilia (Figure 1, a and b). Furthermore, residual cilia that failed to resorb in cells with disassembly induced by ionomycin were nevertheless significantly shortened in reference to cilia in quiescent cells (Figure 1c). Reciprocally, cilia remained at full length in serum-induced cells treated with CMZ (Figure 1c). Conversely, addition of even high levels of calcium to serum-starved cells did not affect the degree of ciliation, indicating that the loss of cilia was specifically related to ionomycin-induced calcium influx rather than high levels of extracellular calcium (Figure 1d).

Calcium/calmodulin activation of AURKA is required for ciliary disassembly

We previously described ciliary disassembly as dependent on AURKA signaling, based on AURKA interactions with NEDD9 and HDAC6 (Pugacheva *et al.*, 2007), and also described AURKA as a Ca^{2+}/CaM target in transient signaling responses (Plotnikova *et al.*, 2010, 2011), suggesting that it may mediate response to ionomycin in ciliary resorption. Indeed, inhibition of AURKA kinase activity using the targeted inhibitor PHA-680632 eliminated ionomycin-induced ciliary resorption (Figure 2a). Cilia not resorbed after 2 h of serum or ionomycin treatment were typically shortened; treatment with the AURKA inhibitor also blocked this shortening (Figure 2). Ionomycin-induced ciliary resorption was also inhibited by small interfering RNA (siRNA)–mediated depletion of AURKA, NEDD9, or HDAC6 (Figure 2c), CMZ and EGTA inhibited serum-induced AURKA activation as effectively as did the AURKA inhibitor PHA-680632 (Figure 2d), and ionomycin activated AURKA at basal bodies as effectively as did serum treatment (Figure 2e). Control of AURKA activation in response to CaM is likely direct, as CaM colocalizes with AURKA at the ciliary basal body (Figure 3a), AURKA coimmunoprecipitates more efficiently with CaM after ionomycin treatment of cells (Figure 3b).

Calcium–calmodulin interactions activate AURKA in mitosis

AURKA activation is required for mitotic entry and AURKA inactivation for resolution of cytokinesis (Glover *et al.*, 1995; Tatsuka *et al.*, 1998; Terada *et al.*, 1998). We found that AURKA activation in lysates prepared from cells synchronized to prometaphase with nocodazole required Ca^{2+} and was inhibited by EGTA (Figure 4a). Further, AURKA was not activated by Ca^{2+} in lysates prepared from G1/S-synchronized cells, suggesting that an earlier priming event was necessary to render cells responsive to Ca^{2+}/CaM (Figure 4a). AURKA activation in mitotic lysates was also dependent on CaM, as preclearance of CaM from mitotic lysates reduced the Ca^{2+}-induced in vitro kinase activity of AURKA subsequently immunoprecipitated from the lysates (Figure 4b). In parallel experiments, synchronization of cells at G1/S or prometaphase followed by release into medium containing CMZ, EGTA, or DMSO for 2 h again indicated that CaM and Ca^{2+} were required for sustained AURKA activation specifically in mitotic cells (Figure 4c). These effects were not secondary consequences of CMZ or EGTA on cell cycle progression, which was comparable in all cases (Figure 4d). AURKA coimmunoprecipitated with CaM more efficiently from M versus quiescent cell lysates (Figure 4e), and AURKA and CaM colocalized during all phases of mitosis, providing suitable physiological context for an interaction (Figure 5).

AURKA activation in mitosis requires interaction with multiple partner proteins, including NEDD9, which associates with the N-terminal unstructured domain of AURKA that contains the primary CaM-binding site (Pugacheva and Golemis, 2005). Significantly, assessment of NEDD9–AURKA interactions with mitotic lysates treated with CMZ or EGTA indicated that CaM and Ca^{2+} were required to sustain interactions between these two proteins (Figure 4f). In a

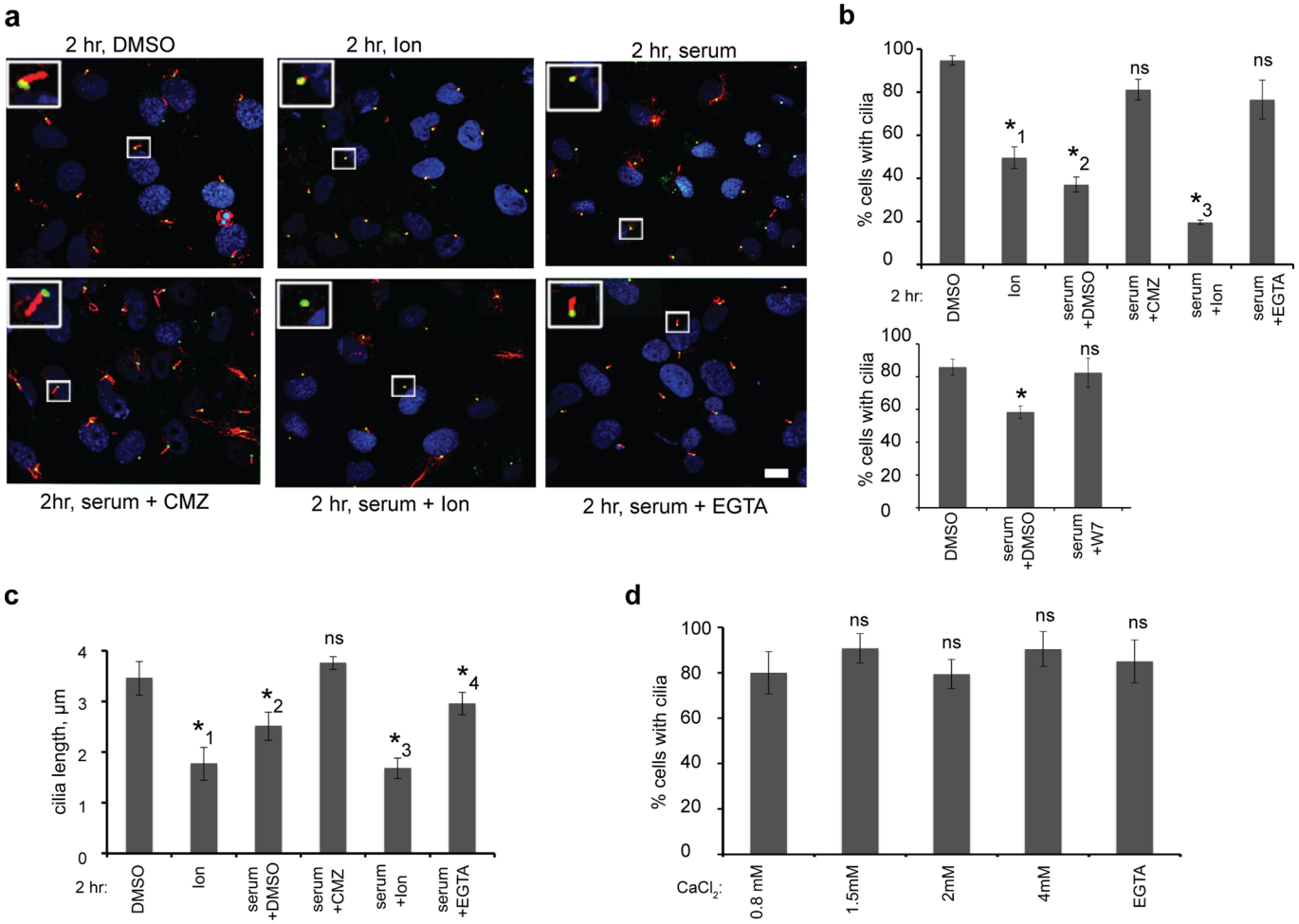

FIGURE 1: Ca^{2+} and CaM are required for ciliary disassembly. (a) Immunofluorescence of cilia in starved hTERT-RPE1 cells treated with 5 µM CaM inhibitor CMZ, 500 nM ionomycin (Ion), 0.5 mM EGTA, or DMSO, with or without serum as indicated. Cilia were visualized with antibodies to acetylated α-tubulin (red) and centrosomes and basal bodies by antibody to γ-tubulin (red); DAPI stains DNA (blue). Scale bar, 10 µm. Insets show magnification of indicated centrosomes and cilia. (b) Top, analysis of data from a, quantifying the percentage of ciliated cells at times before and after the indicated treatments. *1, p = 0.0034; *2, p = 0.0065; *3, p = 0.0079; ns, not significant. Bottom, similar analysis with an independent CaM inhibitor W7 (15 µM) vs. DMSO; here, *p = 0.0003, ns, p > 0.05. An average of 200 cells were counted in each of three experiments; error bars, SE. (c) Analysis of the length of cilia based on immunofluorescence in a. *1, p = 0.0043; *2, p = 0.0056; *3, p = 0.00087; *4, p = 0.0062; ns, not significant. (d) Percentage of ciliated hTERT-RPE1 cells 2 h after addition of indicated concentrations of $CaCl_2$ or 0.5 mM EGTA. ns, not significant. Here 0.8 mM reflects the basal concentration of Ca^{2+} in the Opti-MEM media used for serum starvation. For b–d, an average of 200 cells were counted in each of three experiments; error bars, SE.

complementary experiment, NEDD9 was efficiently pulled down by CaM–Sepharose from total cell lysates (Figure 4g). These data indicated that Ca/CaM binding contributed to the efficiency of kinase-activating interactions between AURKA and at least one of its defined mitotic partners.

Point mutants that disrupt the AURKA–CaM interaction impair AURKA functionality in mitosis

In initial studies of highly transient CaM activation of AURKA in response to endoplasmic reticulum calcium efflux (Plotnikova *et al.*, 2010), we mapped a strong CaM interaction motif to residues 33–89, within the amino-terminus of AURKA, and demonstrated that in vitro incubation of recombinant AURKA with CaM led to autophosphorylation of AURKA on residues S51, S53 or S54, S66 or S67, and S98 (Figure 6a). Among these residues, mitotic phosphorylation on S51 had been independently reported and suggested to protect AURKA from degradation until the end of mitosis (Littlepage and Ruderman, 2002; Littlepage *et al.*, 2002); the other sites were not previously described. We assessed S51A, S53/S54A, S66A/S67A, and S98A mutations, and found that all except S98A significantly disrupted the Ca^{2+}-dependent interaction between CaM and AURKA (Figure 6b). A similar pattern was seen in coprecipitation from mitotic cell lysates (Figure 6c), although partial interaction was retained. All mutations eliminated Ca^{2+}-dependent CaM activation of AURKA in vitro; S51A retained basal AURKA autophosphorylation activity, whereas this was depressed in all other derivatives (Figure 6d).

Fluorescence-activated cell sorting (FACS) analysis of thymidine-synchronized cells overexpressing either red fluorescent protein (RFP)–fused AURKA or its mutated derivatives or RFP control vector (Figure 7a) suggested a modest change in cell cycle progression at 10 h postrelease but few differences after 24 h. This transient change suggested the possibility that cells overexpressing AURKA and

derivatives were being rapidly cleared from the culture. Subsequent live cell imaging to address this possibility indicated that cells overexpressing AURKA and all mutated derivatives except S98A entered mitosis more rapidly than the RFP control (Figure 7b), and over 24 h, a similar number of cells (~40%) entered mitosis for each of the mutations. Among these, 45% of cells overexpressing AURKA failed to exit cytokinesis by completing abscission, consistent with published phenotypes: typically, these cells remained as nonreattaching doublets joined by a thin intracellular bridge and gradually lost cell integrity (Figure 7, c and d). In contrast, none of the mutated derivatives of AURKA produced this terminal phenotype (Figure 7, c and d). Overexpression of S51A, S53A/S54A, and S66A/S67A in each case lead to a high frequency of cells that died between metaphase and anaphase; this phenotype was also seen in ~54% of the cells overexpressing wild-type (WT) AURKA. A less penetrant but similar effect was seen with the S98A-mutated AURKA derivative, with the majority of transfected cells resembling the RFP control. Finally, all AURKA-mutated derivatives retained the ability to localize to centrosomes and the mitotic apparatus, although all were also abundant throughout the cellular cytoplasm (unpublished data). Together these results indicate that mutations at Ca^{2+}/CaM-dependent phosphorylation sites within the minimal strong CaM-interaction domain specifically interfere with AURKA functions associated with mitotic progression rather than initiation of mitosis, whereas mutation of an adjacent site, S98A, nonspecifically impairs AURKA function.

Point mutants that disrupt the AURKA–CaM interaction impair AURKA functionality in ciliary disassembly

Initial use of a similar experimental strategy to evaluate the roles of AURKA mutants in ciliogenesis was unsuccessful because hTERT-RPE1 cells overexpressing AURKA and mutants died during the 48- to 72-h incubation in serum-free medium required for formation of cilia (unpublished data). As an alternative approach, we constructed a panel of hTERT-RPE1 cells with doxycycline (dox)-inducible expression of RFP fused to AURKA or the S51A, S53A/S54A, or S66A/S67A mutated derivatives or RFP vector (Figure 8a). These were used to reexpress AURKA and its derivatives in cells with depleted AURKA, which had an impaired ability to disassemble cilia (Figure 8b) compared to mock-depleted cells. We found that dox induction of RFP-AURKA, but not the S51A-, S53A/S54A-, or S66A/S67A-mutated AURKA derivatives, restored serum-induced ciliary disassembly (Figure 8, c–f). Finally, we confirmed that AURKA and all derivatives appropriately localized to the basal body of the cilia (Figure 8g).

DISCUSSION

In sum, the data in this study for the first time demonstrate that CaM regulation of AURKA is important for normal AURKA function in mitosis, as Ca^{2+}/CaM signaling is necessary for AURKA activation and mutations that disrupt CaM binding to AURKA induce a high frequency of death in cells that fail to progress through anaphase. They also indicate that calcium influx is an essential contributor to ciliary resorption through activity in promoting CaM binding and activation of AURKA and that mutations targeting CaM-AURKA binding impair the ability of AURKA to mediate serum-induced ciliary disassembly. Our data also indicate a novel interaction between CaM and the AURKA activator NEDD9 and show that Ca^{2+}/CaM mediate the AURKA–NEDD9 interaction. Ca^{2+} signaling is known from independent studies to be required for cellular transition from metaphase to anaphase, with inhibition of this signaling triggering the spindle checkpoint (Xu *et al.*, 2003): our data suggest that AURKA may be an essential mediator of these Ca^{2+} signals.

For AURKA, the mutants most potently disrupting activity in mitosis (S51A, S53A/S54A, and S66/S67A) flank a predicted α-helix motif that is in the center of the minimal CaM interaction domain (Plotnikova *et al.*, 2010). Structural analyses of AURKA (Cheetham *et al.*, 2002; Bayliss *et al.*, 2003) demonstrated disorder between residues 1 and 127. In spite of the definition of many known CaM-binding proteins, there is no clear "CaM-binding motif"; however, most CaM-binding domains occur within similarly disordered regions (Radivojac *et al.*, 2006). Functional studies of the AURKA N-terminus have shown that it is dispensable for AURKA interaction with or activation by its mitotic partner TPX2 (Bayliss *et al.*, 2003). However, this domain is required for AURKA localization to centrosomes (Giet and Prigent, 2001), contributes to interactions between AURKA and other activating partners such as NEDD9 (Pugacheva and Golemis, 2005, 2006), and, as noted earlier, contains motifs that control AURKA degradation in mitosis (Littlepage and Ruderman, 2002; Littlepage *et al.*, 2002). Of interest, one study found that a common AURKA polymorphism (V57/I57, located in the center of the CaM-binding region) influences AURKA catalytic activity and intracellular localization and ability of overexpressed AURKA to induce aberrant nuclear morphology, with the I57 variant associated with increased risk of esophageal cancer (Kimura *et al.*, 2005) and earlier age of onset of hereditary nonpolyposis colorectal cancer (Chen *et al.*, 2007). These observations separately support an important functional role of the CaM-binding region. We also noted that overexpression of some of the mutated AURKA derivatives (particularly S66/67A) depressed the basal rate of ciliation in the presence of endogenous AURKA but not in cells with depleted AURKA (compare Figure 8, b and e). Clearly, the role of these CaM-binding sequences requires further study.

AURKA activation in mitosis is supported by dynamic interactions with multiple partner proteins, which besides NEDD9 and TPX2 include PP1 and its inhibitor I-2 (Satinover *et al.*, 2004), PAK1 (Zhao *et al.*, 2005), BORA (Hutterer *et al.*, 2006), and others. We hypothesize that Ca^{2+}-liganded CaM binding induces conformational changes and/or transient phosphorylations in the N-terminal region that influence the association of AURKA with additional proteins that contribute to durable kinase activation. Such an additional level of regulation may help to exactly time AURKA activity during mitotic progression and ciliary resorption. It is also interesting to note that loss of cilia-related structures known as flagella in *Chlamydomonas* has been linked to availability of calcium (Parker and Quarmby, 2003) and is regulated by *Chlamydomonas* Aurora protein kinase, a distant evolutionary relative of AURKA (Pan *et al.*, 2004). Furthermore, the diverse nonmitotic functions now emerging for AURKA include polarity control in postmitotic neurons (Yamada *et al.*, 2010), regulation of interphase microtubules (Lorenzo *et al.*, 2009), and phosphorylation and activation of oncogenic effector proteins such as RALA (Lim *et al.*, 2010) and the androgen receptor (Shu *et al.*, 2010), among others. The likelihood that AURKA is commonly triggered by Ca^{2+}/CaM binding provides an interesting context for the continued investigation of these processes.

Finally, this study for the first time suggests that NEDD9 associates with CaM. Although the primary focus of this study is on the role of NEDD9 in activation of AURKA, NEDD9 (also known as HEF1 and Cas-L) is a scaffold for protein interactions that govern not only cell cycle, but also cell attachment, invasion, survival, and response to hypoxia, and it is itself a prometastatic protein up-regulated and hyperphosphorylated (associated with increased binding activity for some partners) during cancer progression (Law *et al.*, 1999; Fashena *et al.*, 2002; Dadke *et al.*, 2006; Pugacheva and Golemis, 2006; O'Neill *et al.*, 2007; Singh *et al.*, 2007; Izumchenko

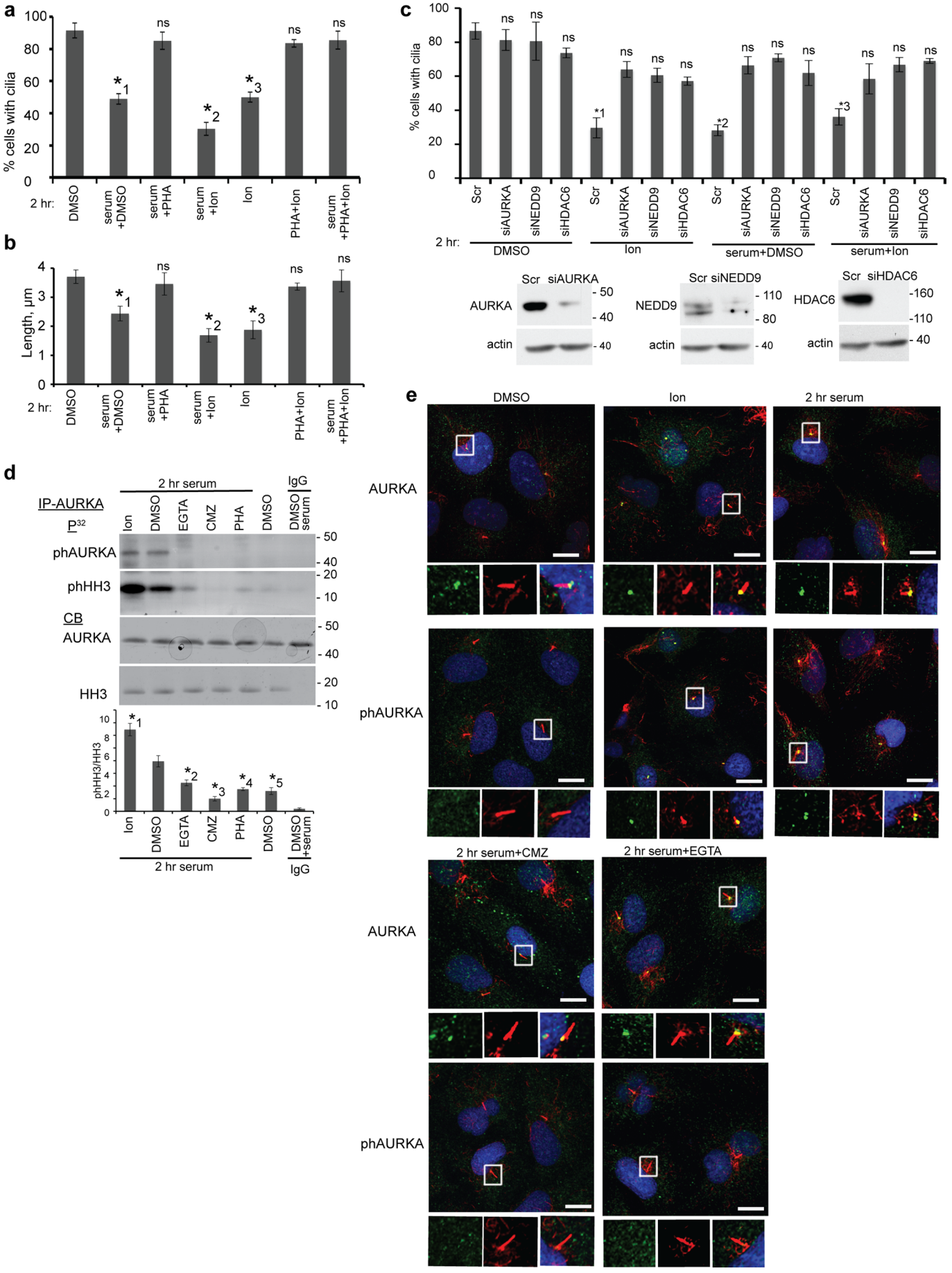
a
% cells with cilia
2 hr:
DMSO
serum +DMSO
serum +PHA
serum +Ion
Ion
PHA+Ion
serum +PHA+Ion
ns
b
Length, µm
c
% cells with cilia
Scr
siAURKA
siNEDD9
siHDAC6
DMSO
Ion
serum+DMSO
serum+Ion
Scr siAURKA
AURKA
actin
Scr siNEDD9
NEDD9
Scr siHDAC6
HDAC6
d
IP-AURKA
P32
2 hr serum
IgG
phAURKA
phHH3
CB
AURKA
HH3
phHH3/HH3
e
DMSO
Ion
2 hr serum
AURKA
phAURKA
2 hr serum+CMZ
2 hr serum+EGTA

et al., 2009). A previous study showed that stimulation of the calcitonin receptor increased intracellular Ca^{2+}, inducing NEDD9 hyperphosphorylation (Zhang *et al.*, 1999). However, this and subsequent work (Zhang *et al.*, 2000) primarily investigated indirect mechanisms through which calcitonin activation signaled through the actin cytoskeleton and linked effectors such as the SRC kinase to activate NEDD9 and did not test the hypothesis of a more direct NEDD9 interaction with machinery for transducing Ca^{2+} signals. Given the many changes in Ca^{2+} signaling that are common in cancer (Roderick and Cook, 2008), our data suggest that CaM–NEDD9 interactions may influence NEDD9 phosphorylation and protein binding profile in tumors, a hypothesis that merits further investigation.

MATERIALS AND METHODS

Plasmids and cell culture

Monomeric RFP (mRFP) was ligated into pcDNA3.1(+) (Invitrogen, Carlsbad, CA) to create pcDNA3.1-mRFP. AURKA and derivatives were expressed from pcDNA3.1-mRFP vectors. Amino acid substitution mutations were introduced into wild-type human *AURKA* cDNA by site-direct mutagenesis, using the QuikChange XL Site-Directed Mutagenesis Kit (Stratagene, La Jolla, CA). Primer sequences are available on request. Tetracycline- or doxycycline-inducible AURKA wild type and mutated derivatives were subcloned into pLUT-lentiviral vector (a gift from Alexey V. Ivanov, WVU, MBRCC), allowing expression as RFP-fused chimeras. 293T packaging cells were used to produce virus and infect the recipient cells. AURKA expression was induced by addition of doxycycline in the medium at a concentration of 1 μg/ml for 6–12 h. HEK293, HeLa, and hTERT-RPE1 cells were maintained in DMEM/F12 with 10% fetal bovine serum (FBS) plus penicillin/streptomycin. We transiently transfected HEK293 cells with expression constructs for *AURKA* using Lipofectamine Plus reagent (Invitrogen), according to the manufacturer's instructions.

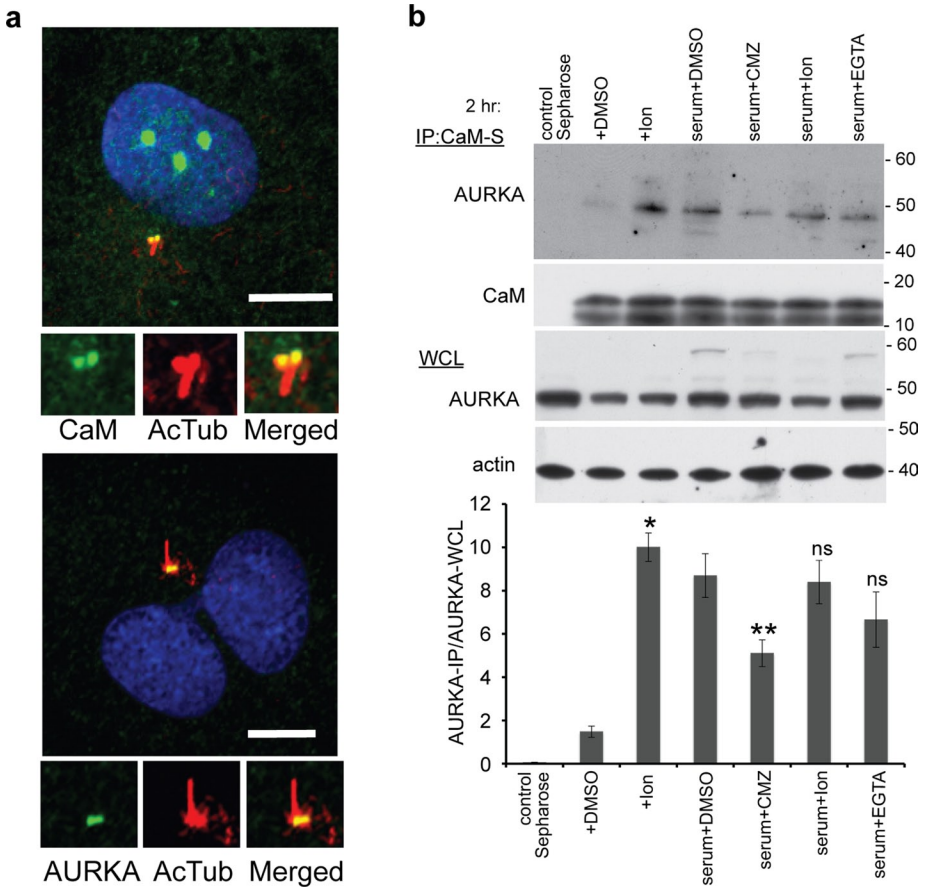

FIGURE 3: Colocalization and coimmunoprecipitation of CaM and AURKA. (a) Immunofluorescence of CaM (green, top) or AURKA (green, bottom), with cilia visualized with antibody to acetylated α-tubulin (red). DAPI indicates nucleus (blue). Scale bar, 10 μm; insets show magnification of cilia and basal body. (b) AURKA was immunoprecipitated with calmodulin–Sepharose (CaM-S) or control Sepharose (S) from starved ciliated hTERT-RPE1 cells treated with 5 μM CaM inhibitor CMZ, 500 nM Ion, 0.5 mM EGTA, or DMSO, with serum as indicated. Graph indicates ratio of immunoprecipitated AURKA to AURKA in WCL, quantified from analysis of three blots; error bars, SE. *p = 0.0016 compared with DMSO control. **p = 0.0003 and ns, not significant, in each case compared with 2 h post serum + DMSO control.

For analysis of ciliary disassembly, hTERT-RPE1 cells were plated at 30% confluence in tissue culture plates containing glass coverslips and starved for 24–48 h in serum-free Opti-MEM to induce cilia formation, followed by treatments described in *Results*. For assessment of AURKA mutants in supporting ciliary disassembly,

FIGURE 2: AURKA, NEDD9, and HDAC6 are intermediates in Ca^{2+}/CaM-induced ciliary disassembly. (a) Ciliated hTERT-RPE1 cells were treated for 2 h with the AURKA inhibitor 0.5 μM PHA-680632 (PHA), 500 nM Ion, or DMSO, with or without the addition of serum as indicated, and then percentage of ciliated cells was assessed after 2 h. *1, p = 0.012; *2, p = 0.032; *3, p = 0.013; ns, not significant. (b) Analysis of the length of cilia based on immunofluorescence in A. *1, p = 0.021; *2, p = 0.0091; *3, p = 0.0016; ns, not significant. (c) Top, percentage of ciliated cells 48 h after transfection with siRNA to AURKA, NEDD9, or HDAC6 or with scrambled (Scr) control siRNA, and treatment for 2 h with 500 nM Ion and/or serum. *1, p = 0.0078; *2, p = 0.014; *3, p = 0.0068; ns, not significant. Bottom, depletion of AURKA, NEDD9, and HDAC6 was confirmed by Western blot. For a–c, an average of 200 cells was counted in each of three experiments; error bars, SE. (d) AURKA activity at 2 h after serum treatment of ciliated cells is induced by treatment with 500 nM Ion or inhibited by treatment with PHA (0.5 μM), CMZ (5 μM), or EGTA (0.5 mM), based on assay of immunoprecipitated AURKA autophosphorylation or phosphorylation of histone H3 (HH3, 3 μg). Graph indicates ratio of phHH3 to total HH3, quantified from analysis of three blots; error bars, SE. *1, p = 0.007; *2, p = 0.0023; *3, p = 0.0094; *4, p = 0.0038; *5, p = 0.0072. Immunoglobulin G (IgG) was used as negative control for immunoprecipitation. (e) hTERT-RPE1 cells were treated with the CaM inhibitor CMZ (5 μM), EGTA (0.5 mM), Ion (500 nM), or DMSO for 2 h, with or without serum as indicated. All images are merged panels of acetylated α-tubulin (red), T^{288}-autophosphorylated (active) phAURKA, or total AURKA (green) and DAPI (blue). Scale bar, 10 μm. Right, magnification of indicated boxed structures.

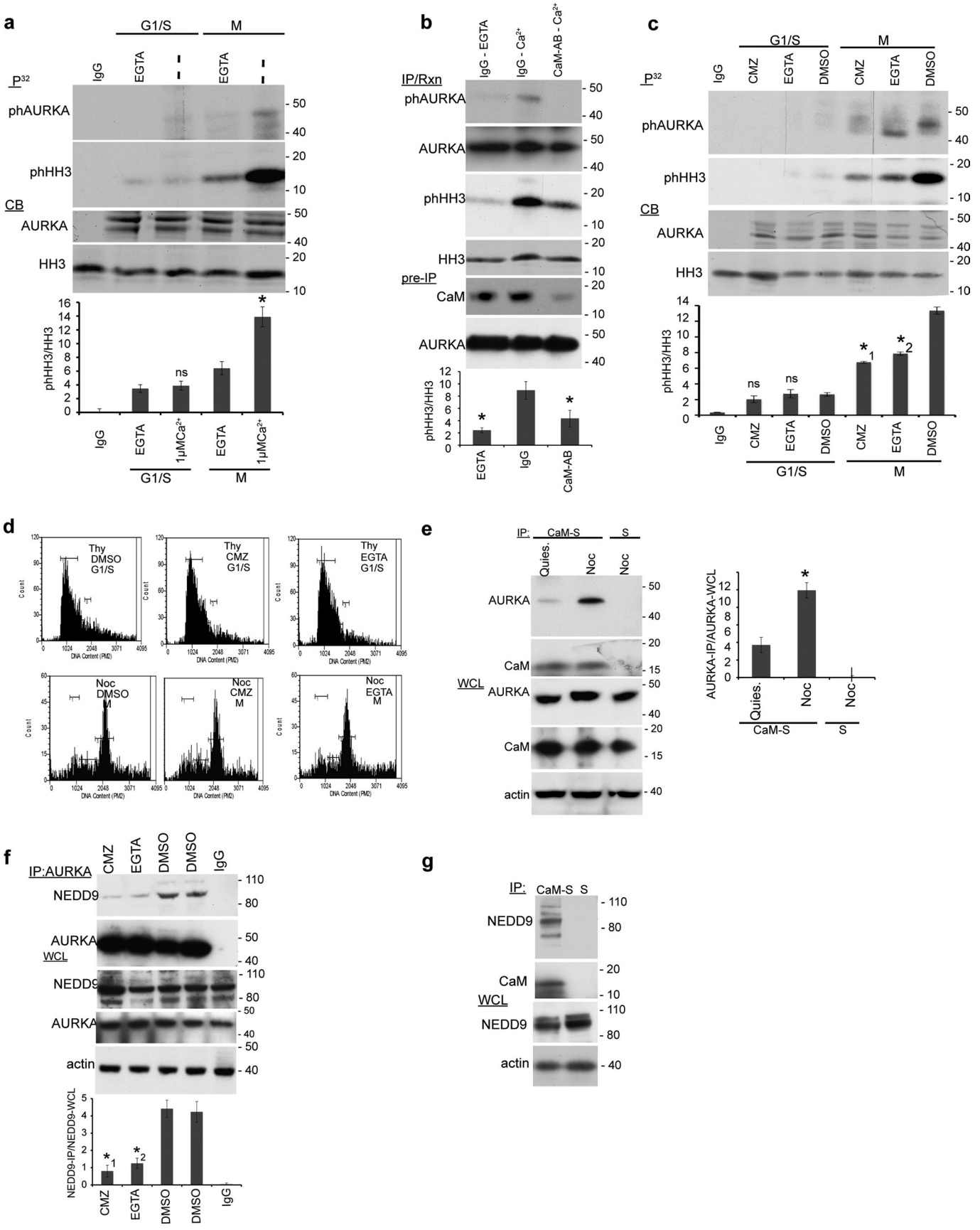

FIGURE 4: Ca^{2+} and CaM are required for activation of Aurora-A in mitosis. (a) In vitro kinase assay with AURKA immunoprecipitated from HEK293 cells synchronized by thymidine in G1/S or by nocodazole in prometaphase (M), then assayed in reactions containing EGTA (0.5 mM) or $CaCl_2$ (1 μM), assessing AURKA or HH3 (HH3) (3 μg) as

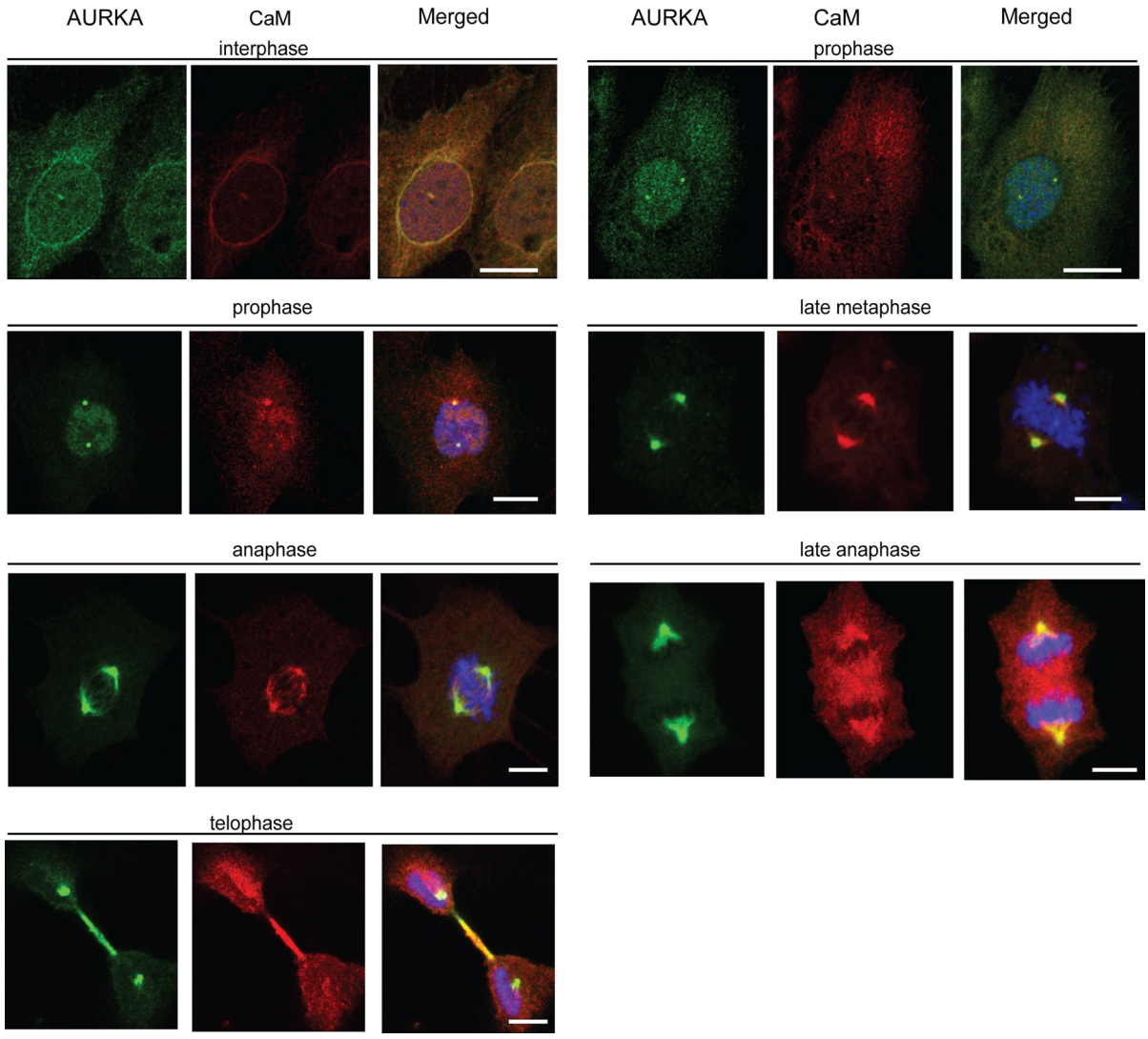

FIGURE 5: Immunofluorescence analysis of localization of AURKA (green) and calmodulin (CaM, red) during mitotic progression. DAPI indicates DNA (blue); scale bar, 10 μm.

substrate, and phosphorylation detected by inclusion of [γ-P^{32}]ATP. Coomassie blue staining indicates total level of proteins in reaction. Graph indicates ratio of phHH3 to total HH3, quantified from analysis of three blots; error bars, SE. * p = 0.017; ns, not significant. IgG was used as negative control for immunoprecipitation. (b) AURKA was immunoprecipitated from mitotic lysates of HEK293 cells pretreated by initial immunoprecipitation with antibodies to CaM (CaM-AB) or control IgG (see pre-IP rows). Kinase assays were performed in the presence of EGTA (0.5 mM) or Ca^{2+} (1 μM), assessing AURKA autophosphorylation, or using HH3 (3 μg) as substrate, with phosphorylation detected by inclusion of [γ-P^{32}]ATP. Graph indicates ratio of phHH3 to total HH3, quantified from analysis of three blots; error bars, SE. *p = 0.0077; ns, not significant. (c) G1/S- and M-phase-synchronized cells were treated for 2 h before lysis with CMZ (5 μM), EGTA (0.5 mM), or control DMSO, and then AURKA was immunoprecipitated and used for in vitro kinase reactions (P^{32} panels), or gels were stained with CB for total level of proteins. Graph indicates ratio of phHH3 to total HH3, quantified from analysis of three blots; error bars, SE; graph quantifies results. *1, p = 0.0069; *2, p = 0.021; ns, not significant. (d) FACS analysis for DNA content for thymidine-blocked HEK293 cells synchronized at the G1/S boundary or in S phase or nocodazole-blocked cells synchronized at G2/M, treated with 2 h with DMSO, CMZ (5 μM), or EGTA (5 mM). (e) AURKA was immunoprecipitated from M-phase, nocodazole-synchronized or serum-starved quiescent lysates (Quies) of HEK293 cells with CaM–Sepharose (CaM-S) or control Sepharose (S). Total protein levels were assessed by Western blotting (WB) with antibodies to AURKA, CaM, or actin. Graph indicates ratio of immunoprecipitated AURKA to AURKA in WCL, quantified from analysis of three blots; error bars, SE. *p = 0.0008. (f) Antibody to AURKA or control IgG was used for immunoprecipitation (IP) from M-synchronized HEK293 cells that were treated for 2 h with CMZ (5 μM), EGTA (0.5 mM), or DMSO, followed by Western blotting with antibodies to NEDD9 or AURKA as indicated. Graph indicates ratio of immunoprecipitated to total NEDD9, quantified from analysis of three blots; error bars, SE. *1, p = 0.0023. *2, p = 0.0035. (g) NEDD9 was immunoprecipitated from WCL with calmodulin-Sepharose (CaM-S) or control Sepharose (S) from 293T cells. Levels of immunoprecipitated and total proteins were assessed by Western blotting (WB).

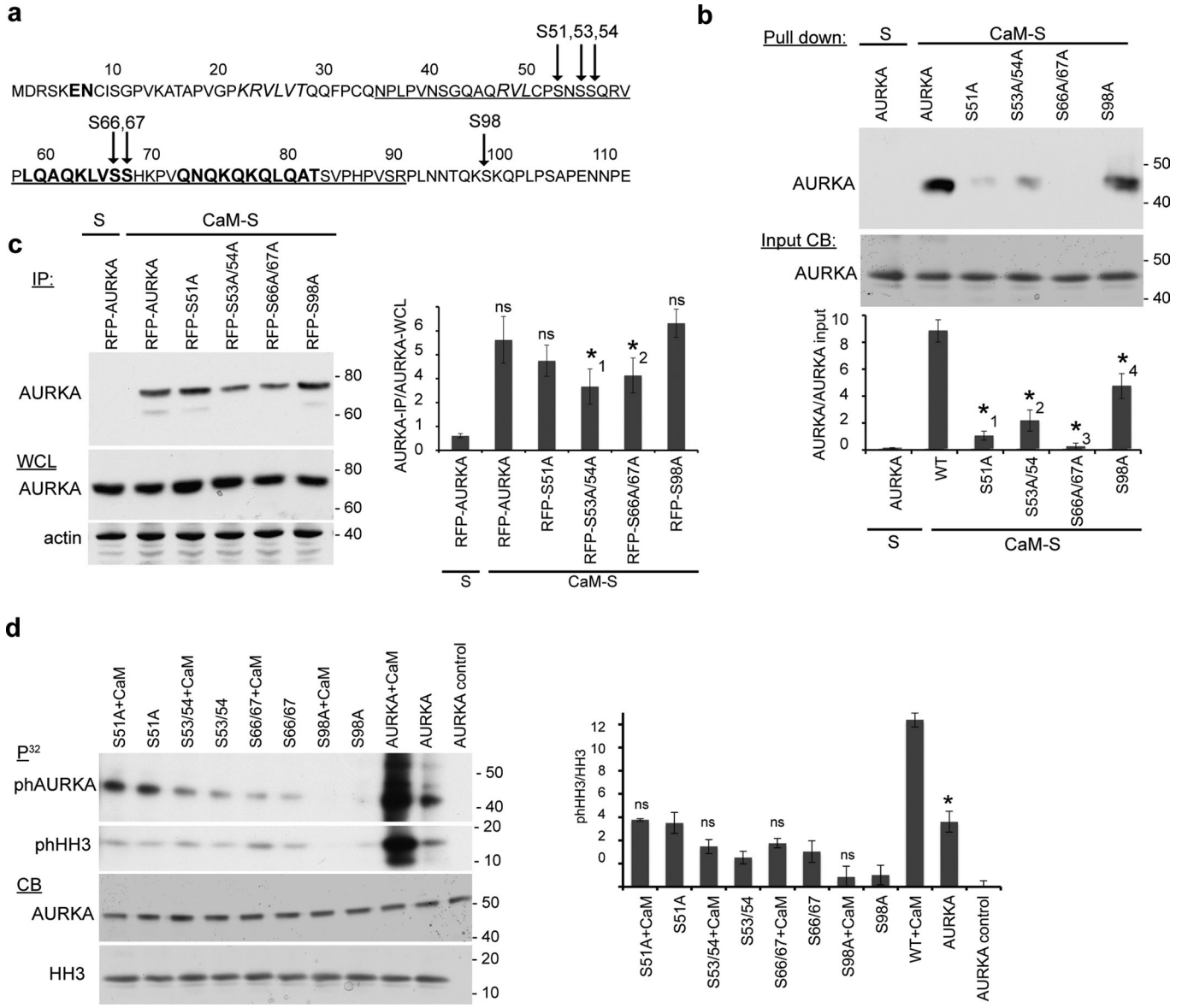

FIGURE 6: CaM-dependent phosphorylation sites on AURKA (S51, S53, S66/S67, S98) contribute to CaM–AURKA binding. (a) Sequence of disordered AURKA N-terminus (residues 1–127). Predicted β-sheets are shown in italics and α-helices in bold. Arrows indicates Ca^{2+}-dependent AURKA autophosphorylation sites. The strong minimal interaction domain (33–89) with CaM is underlined. (b) Calmodulin–Sepharose (CaM-S) or control Sepharose (S) was used in immunoprecipitation of recombinant His-AURKA and indicated mutated derivatives. CB, Coomassie blue staining of starting material. Graph indicates ratio of AURKA bound to CaM-S, quantified from analysis of three blots; error bars, SE. *1, p = 0.0059. *2, p = 0.011. *3, p = 0.017; *4, p = 0.0074. (c) CaM-S or control S were used for IP from WCL expressing RFP-fused AURKA (WT) and indicated mutated derivatives, followed by Western blotting. Graph indicates ratio of AURKA bound to CaM-S, quantified from analysis of three blots; error bars, SE. *1, p = 0.035; *2, p = 0.045; ns, not significant. (d) In vitro kinase assay using recombinant AURK and mutated derivatives, with the addition of CaM as indicated, assessing AURKA autophosphorylation or phosphorylation of histone H3 (HH3) as substrate. AURKA control lane represents reaction without HH3 or ATP. Graph indicates ratio of phHH3 to total HH3, quantified from analysis of three blots; error bars, SE; *p = 0.015; ns, not significant.

two independent siRNAs directed to the 3′ untranslated region (UTR) of AURKA were used to deplete endogenous AURKA (in parallel with a control siRNA) during incubation of cells in serum-free medium to induce cilia. Concurrently, we treated cells with doxycycline or vehicle at 60 h post siRNA transfection, allowing 12 h for production of AURKA or mutated derivatives. Cells were then incubated for 2 h in medium containing serum (to induce disassembly) or without serum and then scored.

Transient transfection of siRNAs was carried out using Lipofectamine RNAiMAX or Oligofectamine transfection reagents (Invitrogen). Cells were assayed 48–72 h after transfection. RNA oligonucleotide duplexes targeted to NEDD9 (Hs_NEDD9_2 [SI00657370], CGCTGCCGAAATGAAGTATAA, and Hs_NEDD9_1 [SI00657363]), AURKA (Hs_STK6_5 [SI03114111] and Hs_AURKA_1_HP, TCCCAGCGCATTCCTTTGCAA [SI00053452], and for 3′ UTR targeting, CCCUCAAUCUAGAACGCUA

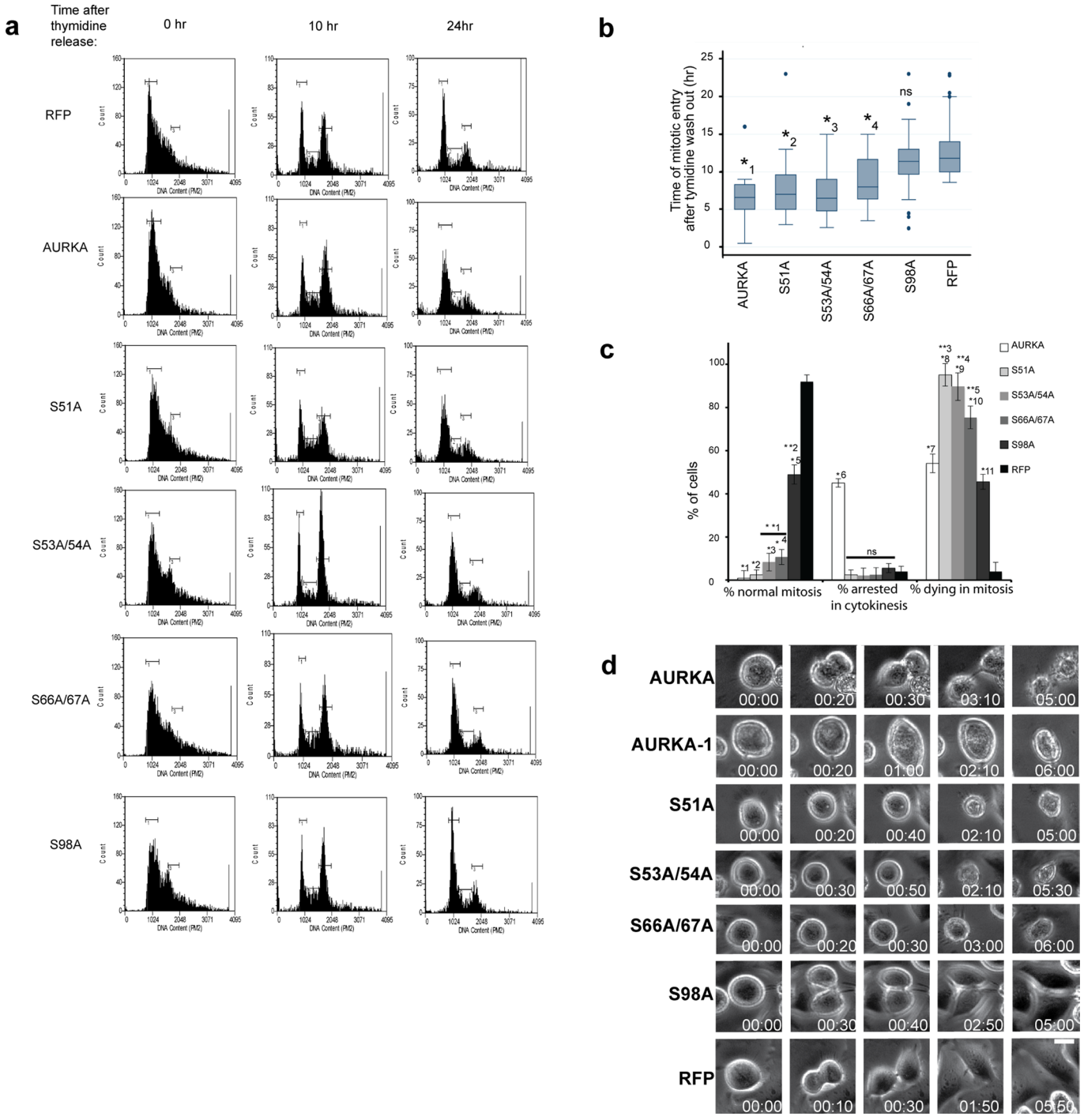

FIGURE 7: Mitotic death in cells overexpressing AURKA CaM-interaction-domain mutants. (a) FACS analysis of DNA content for thymidine-arrested HEK293 cells overexpressing RFP-fused AURKA or mutated derivatives or control RFP at 0, 10, or 24 h after release from block. Horizontal brackets indicate 2N and 4N peaks. (b) Quantitative analysis of movie taken at thymidine-blocked cells transfected with AURKA WT, indicated mutants, and vector pcDNA3.1-RFP. Graph shows time of mitotic entry after release from block. *1, p = 0.0004; *2, p = 0.0001; *3, p = 0.00006; *4, p = 0.0001; ns, not significant; compared with RFP control. An average of 100 cells was counted in each of two movies; the box plots represent the 25th percentile, median (50th percentile), and 75th percentile. (c) Analysis of phenotypes indicated from movie described in b. *1, p = 0.004; *2, p = 0.0026; *3, p = 0.0014; *4, p = 0.0052; *5, p = 0.023; * 6, p = 0.0021; *7, p = 0.0016; *8, p = 0.0036; *9, p = 0.0037; *10, p = 0.0016; *11, p = 0.0037; ns, not significant; compared with RFP control. **1, p = 0.0065; **2, p = 0.016; **3, p = 0.026; **4, p = 0.042; **5, p = 0.015; compared with wild-type AURKA. An average of 100 cells was counted in each of two movies; error bars, SE. (d) Representative images from movies statistically analyzed in b and c. Time 0:00 represents initial rounding after release from thymidine. In each case, the rightmost result, at 5 h postrounding, reflects terminal phenotypes observed for cells (i.e., no reattachment was observed in an additional 7 h of observation; many cells floated off plate). For AURKA, the two predominant terminal phenotypes are shown (AURKA, arrest at cytokinesis; AURKA-1, death between metaphase and anaphase).

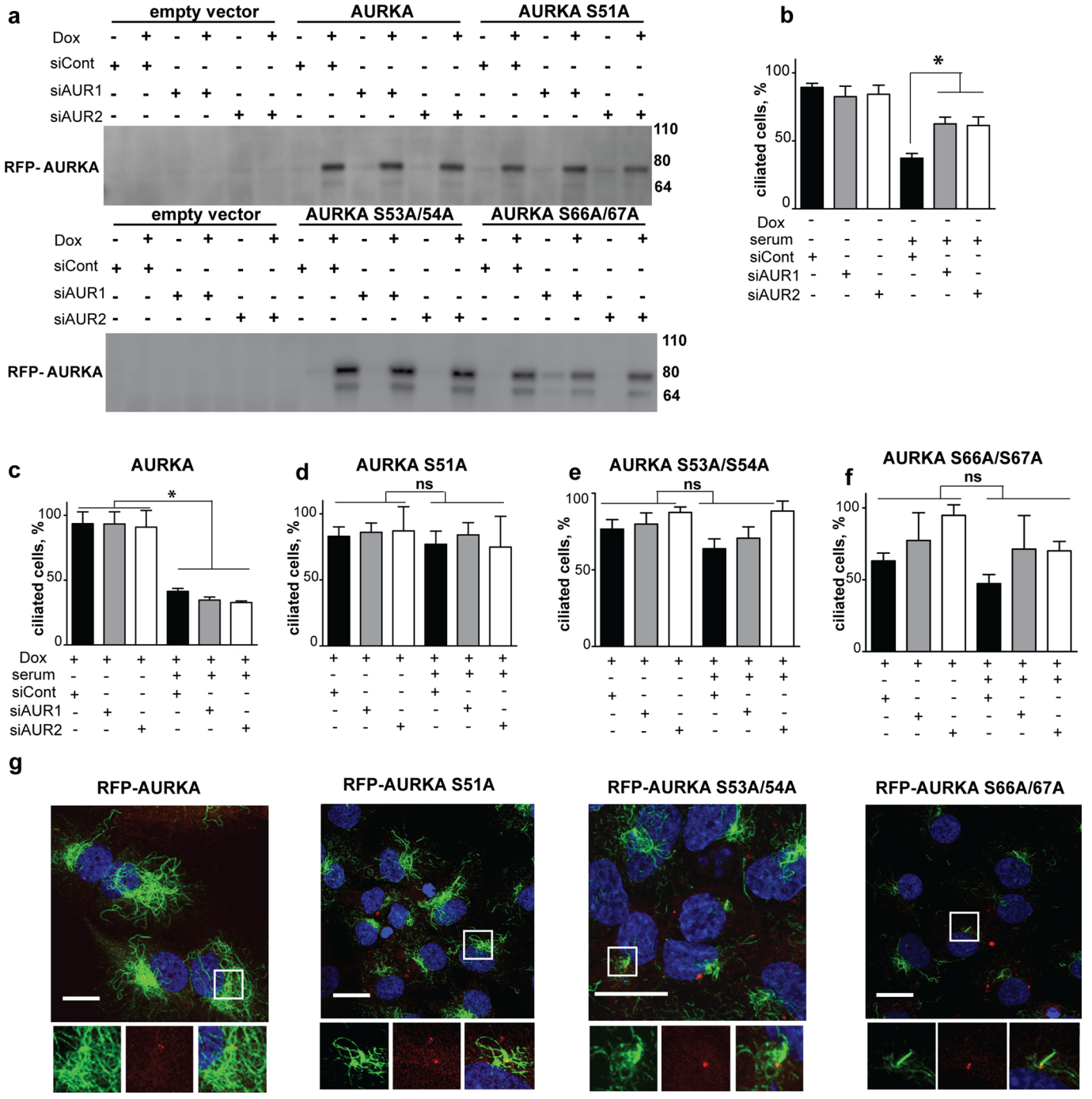

FIGURE 8: Impaired ciliary disassembly in cells expressing AURKA CaM-interaction-domain mutants. (a) Expression of dox-induced RFP-AURKA and AURKA derivatives in the context of AURKA depleted by two independent siRNAs (siAUR1, siAUR2), or control depleted (siCont), in the presence or absence of dox. (b) Percentage of ciliated cells 2 h after serum induction of ciliary disassembly for cells grown in the absence of doxycycline (dox) after treatment with siRNA to deplete AURKA, or control siRNA. *p = 0.001. (c–f) Percentage of ciliated cells 2 h after serum induction of ciliary disassembly for cells grown in the presence of dox to induce expression of AURKA (c), S51A (d), S53A/S54A (e), or S66A/S67A (f). Statistical comparisons represent plus vs. minus serum conditions for each siRNA. *p < 0.001; ns, nonspecific. (g) Immunofluorescence of RFP-AURKA and indicated derivatives at base of cilia. Red, RFP-AURKA or mutated AURKA (as indicated); green, acetylated α-tubulin; blue, DAPI. Scale bar, 20 μm.

[D-003545-35-0005, siAUR1] and CGGUAGGCCUGAUUGGGUU [J-003545-27-0005, siAUR2]) and HDAC6 (GGGAGGUUCUUGUGAGAUC [J-003499-05] and GUUCACAGCCUAGAAUAUA [J-003499-08]) were purchased from Qiagen (Valencia, CA) or Thermo Scientific (Waltham, MA; HDAC6, 3′ UTR-targeting AURKA), as well as scrambled negative controls. After transfection of siRNAs, degree of depletion of target proteins was determined by Western blot.

Immunofluorescence microscopy and live cell imaging

Cells growing on coverslips were fixed with 4% paraformaldehyde (10 min) and then cold methanol (5 min), permeabilized with 1%Triton X-100 in phosphate-buffered saline (PBS), blocked in 1× PBS with 3–5% BSA, and incubated with antibodies using standard protocols. Alternatively, to maximize clear signals at centrosomes, cells were fixed in cold methanol (–20°C) for 2 min, blocked, and incubated with antibody. Primary antibodies included mouse anti-AURKA (BD Biosciences, San Jose, CA), rabbit anti-AURKA, rabbit polyclonal anti–phospho-AURKA/T288 (Cell Signaling, Beverly, MA), anti–acetylated α-tubulin monoclonal antibody (mAb; clone 6-11B-1; Sigma-Aldrich, St. Louis, MO, and clone K(Ac)40, Biomol International, Enzo Life Sciences, Plymouth, PA), monoclonal anti-calmodulin (Santa Cruz Biotechnology, Santa Cruz, CA, and Millipore, Billerica, MA), and mouse anti–γ-tubulin mAb (Sigma-Aldrich). Secondary antibodies labeled with Alexa 488, Alexa 568, and 4′,6-diamidino-2-phenylindole (DAPI) to stain DNA were from Molecular Probes/Invitrogen (Carlsbad, CA). Confocal microscopy was performed using a Nikon C1 Spectral confocal microscope (Nikon, Melville, NY) equipped with a numerical aperture (NA) 1.40, oil immersion, 63× Plan Apo objective (Nikon). Images were acquired at room temperature using EZ-C1 3.8 (Nikon) software and analyzed using MetaMorph (Molecular Devices, Union City, CA) and Photoshop, version CS2 (Adobe, San Jose, CA) software. Adjustments to brightness and contrast were minimal and were applied to the whole image.

For live cell imaging, transfected HEK293 cells expressing RFP-AURKA, RFP-fused AURKA mutants, or RFP were incubated for 18 h with 2 mM thymidine, washed twice in PBS, then returned to fresh medium and observed for 24 h. Videos of RFP-positive cells were captured with an Inverted Nikon TE300, equipped for phase and epifluorescence with a Ludl MAC2000 *x-y* stage control and *z*-axis motor (Nikon) and a Spot RT (Diagnostic Instruments, Sterling Heights, MI) monochrome camera (12-bit images) using a 20× Plan Fluor, NA 0.45, ELWD, WD 7.4 objective. Image processing was performed using MetaMorph software as described in the manufacturer's guidebook. MetaVue (Molecular Devices) software was used for processing and analysis of immunofluorescent images.

Protein expression, Western blotting, and immunoprecipitation

Recombinant hexahistidine wild-type and mutant AURKA were produced in a baculovirus expression system at the Recombinant Protein Facility at the Wistar Institute (Philadelphia, PA). For Western blotting and immunoprecipitation, mammalian cells were disrupted in CelLytic M lysis buffer (Sigma-Aldrich) supplemented with protease and phosphatase inhibitor cocktails (Roche, Basel, Switzerland). Whole cell lysates were used either directly for SDS–PAGE or for immunoprecipitation. Immunoprecipitation samples were incubated overnight with antibody at 4°C and subsequently incubated for 2 h with protein A/G–Sepharose (Pierce, Rockford, IL), washed, and resolved by SDS–PAGE.

For detection of binding with CaM, cell lysates in lysis buffer (PBS with 1% Triton X-100) or purified proteins were diluted in binding buffer (50 mM Tris-HCl, pH 7.6,120 mM NaCl, 2 mM $CaCl_2$, 1% Brij) and incubated with Calmodulin-Sepharose 4B (GE Healthcare, Piscataway, NJ) or control Sepharose for 3–4 h at 4°C as indicated in the figure legends. After washing, beads were boiled in SDS sample buffer and separated by SDS–PAGE followed by Western blotting.

Western blotting was done using standard procedures. Primary antibodies included mouse anti-NEDD9 mAb (clone 2G9; Pugacheva and Golemis, 2005), anti-AURKA (BD Biosciences, San Jose, CA), anti–phospho-AURKA-T^{288} (Cell Signaling), polyclonal anti-HDAC6 (Millipore), monoclonal anti-calmodulin (Millipore), and anti–β-actin mAb (AC15; Sigma-Aldrich). Polyclonal anti-AURKA agarose–immobilized conjugate (Bethyl, Montgomery, TX) was used for immunoprecipitations. Secondary anti-mouse and anti-rabbit horseradish peroxidase–conjugated antibodies (GE Healthcare) were used at a dilution of 1:10,000 for visualization of Western blots and blots developed by chemiluminescence using the West-Pico system (Pierce). Image analysis was done using ImageJ (National Institutes of Health, Bethesda, MD), with signal intensity normalized to β-actin or total level of detected proteins.

Phosphorylation assays

Histone H3 (Upstate, Charlottesville, VA) was used as substrate for AURKA phosphorylation, using standard methods. Parallel aliquots without [γ-^{32}P]ATP were processed for SDS–PAGE/Coomassie blue staining (Invitrogen). To assess calcium and CaM-dependent Aurora-A activation, we performed the in vitro kinase assay using AURKA purified from baculovirus or according to the protocol described in the *Protein expression, Western blotting, and immunoprecipitation* section in the presence of 1 μM CaM (Calbiochem, La Jolla, CA) with 1 mM Ca^{2+} or with 1 mM EGTA.

Cell cycle synchronization

Cells were incubated for 18 h with 2 mM thymidine, washed twice in PBS, and then either assayed directly (for observation at the G1/S boundary) or returned to fresh medium and allowed to grow for 9–12 h to observe synchronized progression to mitosis. Alternatively, to obtain an M-phase cell population, cells were synchronized by 2 mM nocodazole for 16 h, and rounded cells were collected by shakeoff. Collected cells were suspended in fresh DMEM containing 10% FBS and analyzed at 0 and 30 min after release. For all synchronization procedures, the predicted cell cycle progression was confirmed by flow cytometry analysis using Guava (Millipore), with data analyzed using the Guava Cell Cycle Software for the EasyCyte Plus System (Millipore).

Statistical analysis

Statistical comparisons were made using a two-tailed Student's *t* test. Experimental values were reported as the means ± SE. Differences in mean values were considered significant at $p < 0.05$. For multiple group comparison, repeated-measures analysis of variance (ANOVA) was used to analyze the p values and the significance of the difference between the groups. A value of $p < 0.0001$ for each group with a significant difference is labeled by double or triple asterisks. The ANOVA test was followed by Tukey's test, with a significance level 0.01. All calculations of statistical significance were made using InStat software (GraphPad, San Diego, CA).

ACKNOWLEDGMENTS

This work was supported by grant R01 CA63366 and Pennsylvania Tobacco Settlement funding (to E.A.G.), grants R01 CA148671 and KG 100539 (to E.N.P.), and National Institutes of Health Core Grant CA06927 and the Pew Charitable Fund (to Fox Chase Cancer Center [FCCC]). We are grateful to Andrey Efimov from the Cell Imaging Facility (Biological Imaging Facility, FCCC), to Neil Beeharry for help with the movies, and to Brian Egleston from Biostatistics (FCCC) for help with analysis.

REFERENCES

Bayliss R, Sardon T, Vernos I, Conti E (2003). Structural basis of Aurora-A activation by TPX2 at the mitotic spindle. Mol Cell 12, 851–862.

Berdnik D, Knoblich JA (2002). *Drosophila* Aurora-A is required for centrosome maturation and actin-dependent asymmetric protein localization during mitosis. Curr Biol 12, 640–647.
Carmena M, Ruchaud S, Earnshaw WC (2009). Making the Auroras glow: regulation of Aurora A and B kinase function by interacting proteins. Curr Opin Cell Biol 21, 796–805.
Carol H *et al.* (2011). Efficacy and pharmacokinetic/pharmacodynamic evaluation of the Aurora kinase A inhibitor MLN8237 against preclinical models of pediatric cancer. Cancer Chemother Pharmacol 68, 1291–1304.
Cheetham GM, Knegtel RM, Coll JT, Renwick SB, Swenson L, Weber P, Lippke JA, Austen DA (2002). Crystal structure of aurora-2, an oncogenic serine/threonine kinase. J Biol Chem 277, 42419–42422.
Chen J, Sen S, Amos CI, Wei C, Jones JS, Lynch P, Frazier ML (2007). Association between Aurora-A kinase polymorphisms and age of onset of hereditary nonpolyposis colorectal cancer in a Caucasian population. Mol Carcinog 46, 249–256.
Dadke D, Jarnik M, Pugacheva EN, Singh MK, Golemis EA (2006). Deregulation of HEF1 impairs M-phase progression by disrupting the RhoA activation cycle. Mol Biol Cell 17, 1204–1217.
Dodson CA, Bayliss R (2012). Activation of Aurora-A kinase by protein partner binding and phosphorylation are independent and synergistic. J Biol Chem 287, 1150–1157.
Eyers PA, Erikson E, Chen LG, Maller JL (2003). A novel mechanism for activation of the protein kinase Aurora A. Curr Biol 13, 691–697.
Fashena SJ, Einarson MB, O'Neill GM, Patriotis CP, Golemis EA (2002). Dissection of HEF1-dependent functions in motility and transcriptional regulation. J Cell Sci 115, 99–111.
Gautschi O, Heighway J, Mack PC, Purnell PR, Lara PN Jr, Gandara DR (2008). Aurora kinases as anticancer drug targets. Clin Cancer Res 14, 1639–1648.
Giet R, Prigent C (2001). The non-catalytic domain of the *Xenopus laevis* auroraA kinase localises the protein to the centrosome. J Cell Sci 114, 2095–2104.
Glover DM, Leibowitz MH, McLean DA, Parry H (1995). Mutations in aurora prevent centrosome separation leading to the formation of monopolar spindles. Cell 81, 95–105.
Hannak E, Kirkham M, Hyman AA, Oegema K (2001). Aurora-A kinase is required for centrosome maturation in *Caenorhabditis elegans*. J Cell Biol 155, 1109–1116.
Hutterer A, Berdnik D, Wirtz-Peitz F, Zigman M, Schleiffer A, Knoblich JA (2006). Mitotic activation of the kinase Aurora-A requires its binding partner Bora. Dev Cell 11, 147–157.
Izumchenko E *et al.* (2009). NEDD9 promotes oncogenic signaling in mammary tumor development. Cancer Res 69, 7198–7206.
Kashatus DF, Lim KH, Brady DC, Pershing NL, Cox AD, Counter CM (2011). RALA and RALBP1 regulate mitochondrial fission at mitosis. Nat Cell Biol 13, 1108–1115.
Kimura MT, Mori T, Conroy J, Nowak NJ, Satomi S, Tamai K, Nagase H (2005). Two functional coding single nucleotide polymorphisms in STK15 (Aurora-A) coordinately increase esophageal cancer risk. Cancer Res 65, 3548–3554.
Kinzel D *et al.* (2010). Pitchfork regulates primary cilia disassembly and left-right asymmetry. Dev Cell 19, 66–77.
Law SF, Zhang Y-Z, Fashena S, Toby G, Estojak J, Golemis EA (1999). Dimerization of the docking/adaptor protein HEF1 via a carboxy-terminal helix-loop-helix domain. Exp Cell Res 252, 224–235.
Lim KH, Brady DC, Kashatus DF, Ancrile BB, Der CJ, Cox AD, Counter CM (2010). Aurora-A phosphorylates, activates, and relocalizes the small GTPase RalA. Mol Cell Biol 30, 508–523.
Littlepage LE, Ruderman JV (2002). Identification of a new APC/C recognition domain, the A box, which is required for the Cdh1-dependent destruction of the kinase Aurora-A during mitotic exit. Genes Dev 16, 2274–2285.
Littlepage LE, Wu H, Andresson T, Deanehan JK, Amundadottir LT, Ruderman JV (2002). Identification of phosphorylated residues that affect the activity of the mitotic kinase Aurora-A. Proc Natl Acad Sci USA 99, 15440–15445.
Lorenzo C, Liao Q, Hardwicke MA, Ducommun B (2009). Pharmacological inhibition of aurora-A but not aurora-B impairs interphase microtubule dynamics. Cell Cycle 8, 1733–1737.
Manfredi MG *et al.* (2011). Characterization of Alisertib (MLN8237), an investigational small molecule inhibitor of aurora A kinase using novel in vivo pharmacodynamic assays. Clin Cancer Res 17, 7614–7624.
Marumoto T, Zhang D, Saya H (2005). Aurora-A—a guardian of poles. Nat Rev Cancer 5, 42–50.
Mori D, Yamada M, Mimori-Kiyosue Y, Shirai Y, Suzuki A, Ohno S, Saya H, Wynshaw-Boris A, Hirotsune S (2009). An essential role of the aPKC-Aurora A-NDEL1 pathway in neurite elongation by modulation of microtubule dynamics. Nat Cell Biol 11, 1057–1068.
O'Neill GM, Seo S, Serebriiskii IG, Lessin SR, Golemis EA (2007). A new central scaffold for metastasis: parsing HEF1/Cas-L/NEDD9. Cancer Res 67, 8975–8979.
Pan J, Wang Q, Snell WJ (2004). An aurora kinase is essential for flagellar disassembly in *Chlamydomonas*. Dev Cell 6, 445–451.
Parker JD, Quarmby LM (2003). *Chlamydomonas* fla mutants reveal a link between deflagellation and intraflagellar transport. BMC Cell Biol 4, 11.
Plotnikova OV, Golemis EA, Pugacheva EN (2008). Cell cycle-dependent ciliogenesis and cancer. Cancer Res 68, 2058–2061.
Plotnikova OV, Pugacheva E, Golemis EA (2011). Aurora-A kinase activity influences calcium signaling in kidney cells. J Cell Biol 193, 1021–1032.
Plotnikova OV, Pugacheva EN, Dunbrack RL, Golemis EA (2010). Rapid calcium-dependent activation of Aurora-A kinase. Nat Commun 1, 64.
Pugacheva EN, Golemis EA (2005). The focal adhesion scaffolding protein HEF1 regulates activation of the Aurora-A and Nek2 kinases at the centrosome. Nat Cell Biol 7, 937–946.
Pugacheva EN, Golemis EA (2006). HEF1-aurora A interactions: points of dialog between the cell cycle and cell attachment signaling networks. Cell Cycle 5, 384–391.
Pugacheva EN, Jablonski SA, Hartman TR, Henske EP, Golemis EA (2007). HEF1-dependent Aurora A activation induces disassembly of the primary cilium. Cell 129, 1351–1363.
Radivojac P, Vucetic S, O'Connor TR, Uversky VN, Obradovic Z, Dunker AK (2006). Calmodulin signaling: analysis and prediction of a disorder-dependent molecular recognition. Proteins 63, 398–410.
Roderick HL, Cook SJ (2008). Ca2+ signalling checkpoints in cancer: remodelling Ca2+ for cancer cell proliferation and survival. Nat Rev Cancer 8, 361–375.
Satinover DL, Leach CA, Stukenberg PT, Brautigan DL (2004). Activation of Aurora-A kinase by protein phosphatase inhibitor-2, a bifunctional signaling protein. Proc Natl Acad Sci USA 101, 8625–8630.
Shu SK, Liu Q, Coppola D, Cheng JQ (2010). Phosphorylation and activation of androgen receptor by Aurora-A. J Biol Chem 285, 33045–33053.
Singh M, Cowell L, Seo S, O'Neill G, Golemis E (2007). Molecular basis for HEF1/NEDD9/Cas-L action as a multifunctional co-ordinator of invasion, apoptosis and cell cycle. Cell Biochem Biophys 48, 54–72.
Tatsuka M, Katayama H, Ota T, Tanaka T, Odashima S, Suzuki F, Terada Y (1998). Multinuclearity and increased ploidy caused by overexpression of the aurora- and Ipl1-like midbody-associated protein mitotic kinase in human cancer cells. Cancer Res 58, 4811–4816.
Terada Y, Tatsuka M, Suzuki F, Yasuda Y, Fujita S, Otsu M (1998). AIM-1: a mammalian midbody-associated protein required for cytokinesis. EMBO J 17, 667–676.
Toya M, Terasawa M, Nagata K, Iida Y, Sugimoto A (2011). A kinase-independent role for Aurora A in the assembly of mitotic spindle microtubules in *Caenorhabditis elegans* embryos. Nat Cell Biol 13, 710–716.
Wu JC, Chen TY, Yu CT, Tsai SJ, Hsu JM, Tang MJ, Chou CK, Lin WJ, Yuan CJ, Huang CY (2005). Identification of V23RalA-Ser194 as a critical mediator for Aurora-A-induced cellular motility and transformation by small pool expression screening. J Biol Chem 280, 9013–9022.
Xu N, Luo KQ, Chang DC (2003). Ca2+ signal blockers can inhibit M/A transition in mammalian cells by interfering with the spindle checkpoint. Biochem Biophys Res Commun 306, 737–745.
Yamada M, Hirotsune S, Wynshaw-Boris A (2010). The essential role of LIS1, NDEL1 and Aurora-A in polarity formation and microtubule organization during neurogenesis. Cell Adh Migr 4, 180–184.
Yang H, He L, Kruk P, Nicosia SV, Cheng JQ (2006). Aurora-A induces cell survival and chemoresistance by activation of Akt through a p53-dependent manner in ovarian cancer cells. Int J Cancer 119, 2304–2312.
Zhang Z, Baron R, Horne WC (2000). Integrin engagement, the actin cytoskeleton, and c-Src are required for the calcitonin-induced tyrosine phosphorylation of paxillin and HEF1, but not for calcitonin-induced Erk1/2 phosphorylation. J Biol Chem 275, 37219–37223.
Zhang Z, Hernandez-Lagunas L, Horne WC, Baron R (1999). Cytoskeleton-dependent tyrosine phosphorylation of the p130(Cas) family member HEF1 downstream of the G protein-coupled calcitonin receptor. Calcitonin induces the association of HEF1, paxillin, and focal adhesion kinase. J Biol Chem 274, 25093–25098.
Zhao ZS, Lim JP, Ng YW, Lim L, Manser E (2005). The GIT-associated kinase PAK targets to the centrosome and regulates Aurora-A. Mol Cell 20, 237–249.